Detection of waves in the equatorial coronal holes

D. Banerjee

Indian Institute of Astrophysics

E.O'Shea & J.G. Doyle

(Armagh Observatory)

Motivation

Coronal Holes (CH) ⇒

Source region of the Fast Solar Wind

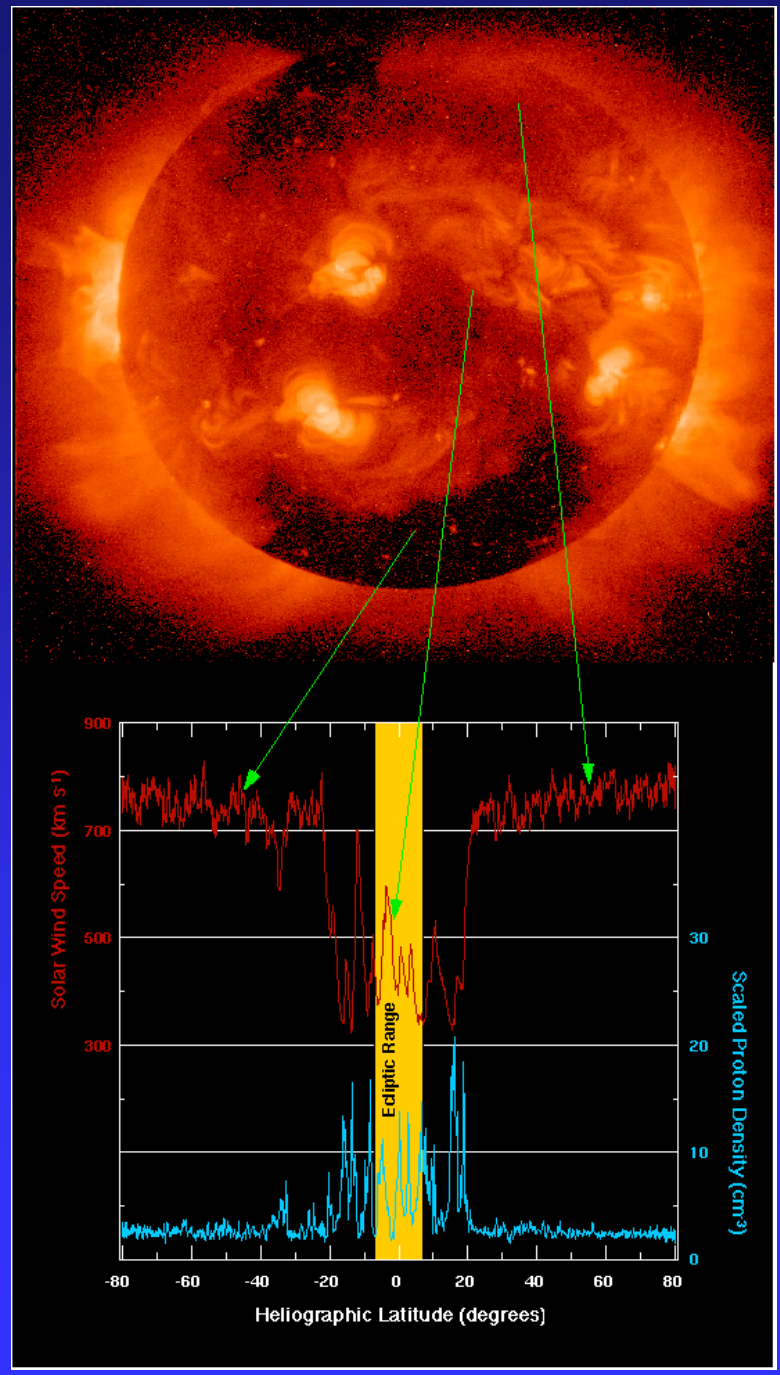

Solar wind originates in coronal funnels

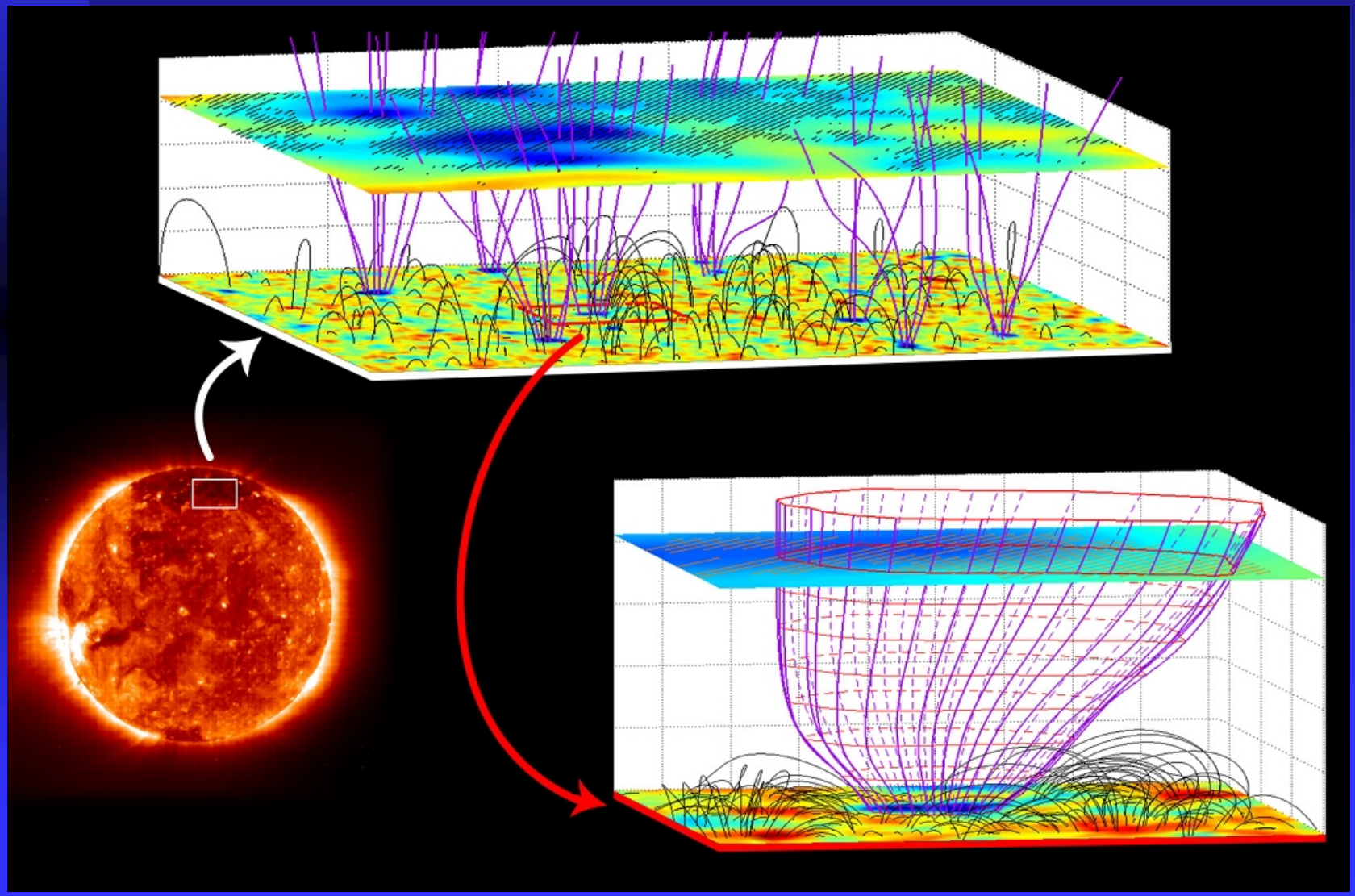

Observational log:

- Coronal Diagnostic spectrometer (CDS/SoHO)
- Long temporal series sequence for 11 TR and coronal lines formed between 2.5 x 10^5 to 2.5 x 10^6 K.
- We will present only results from

  O v 629Å (2.5 x 10^5) , coronal line Mg x 624 Å
- Slit width 4 x 240 arc sec
- Exposure time 60 sec

Dataset	Location	Start time
s26412r00	Eq. CH	07-12-02 12:22
s26412r01	Eq. CH	07-12-02 15:13
s26431r00	Eq. CH	10-12-02 16:26
s26431r00	Eq. CH	10-12-02 19:17
s26435r00	NP CH	11-12-02 06:33
s26502r00	SP CH	20-12-02 18:00
s26502r01	SP CH	20-12-02 20:50

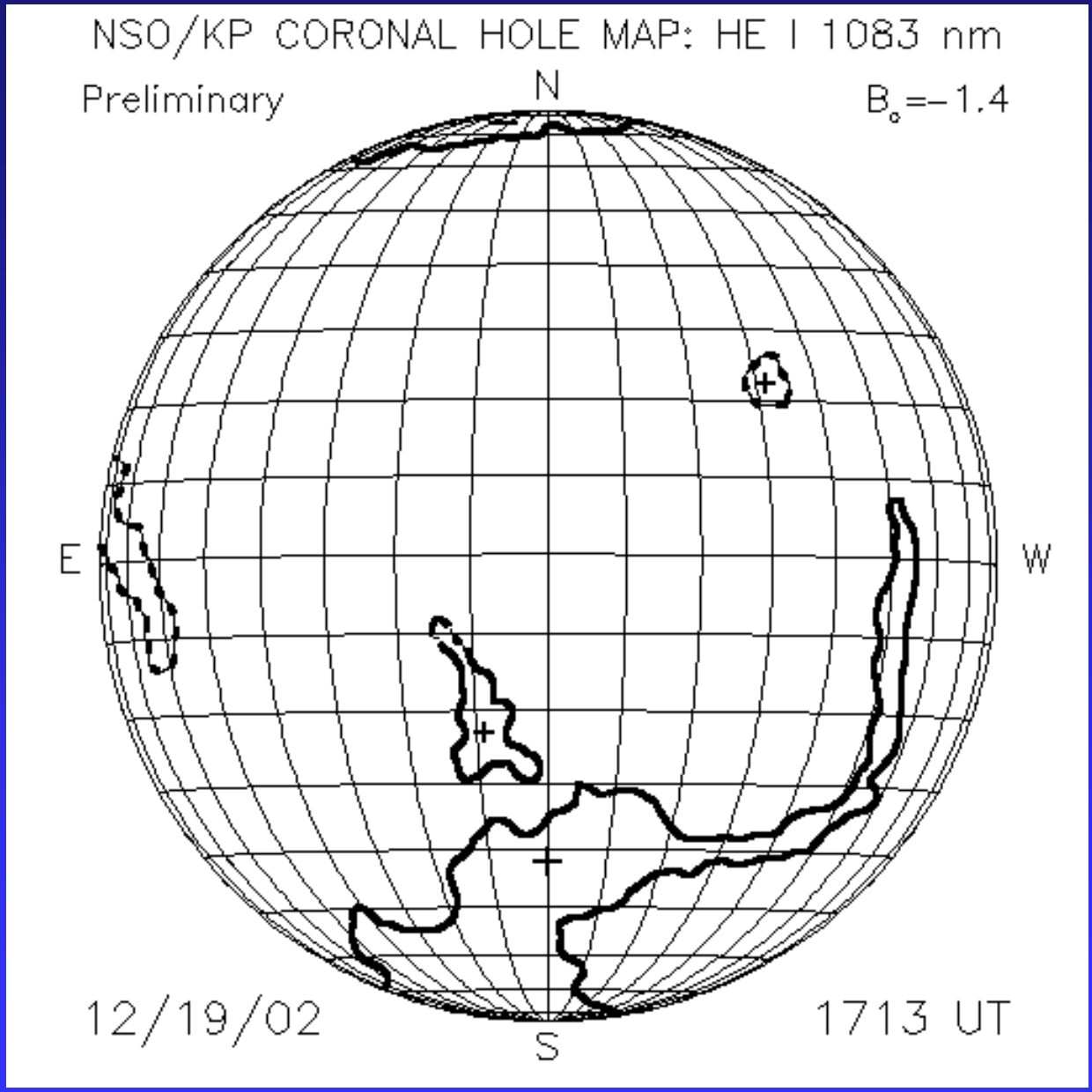
NSO/KP CORONAL HOLE MAP: HE I 1083 nm
Preliminary
N
B_o=–1.4
E
W
S
12/19/02
1713 UT

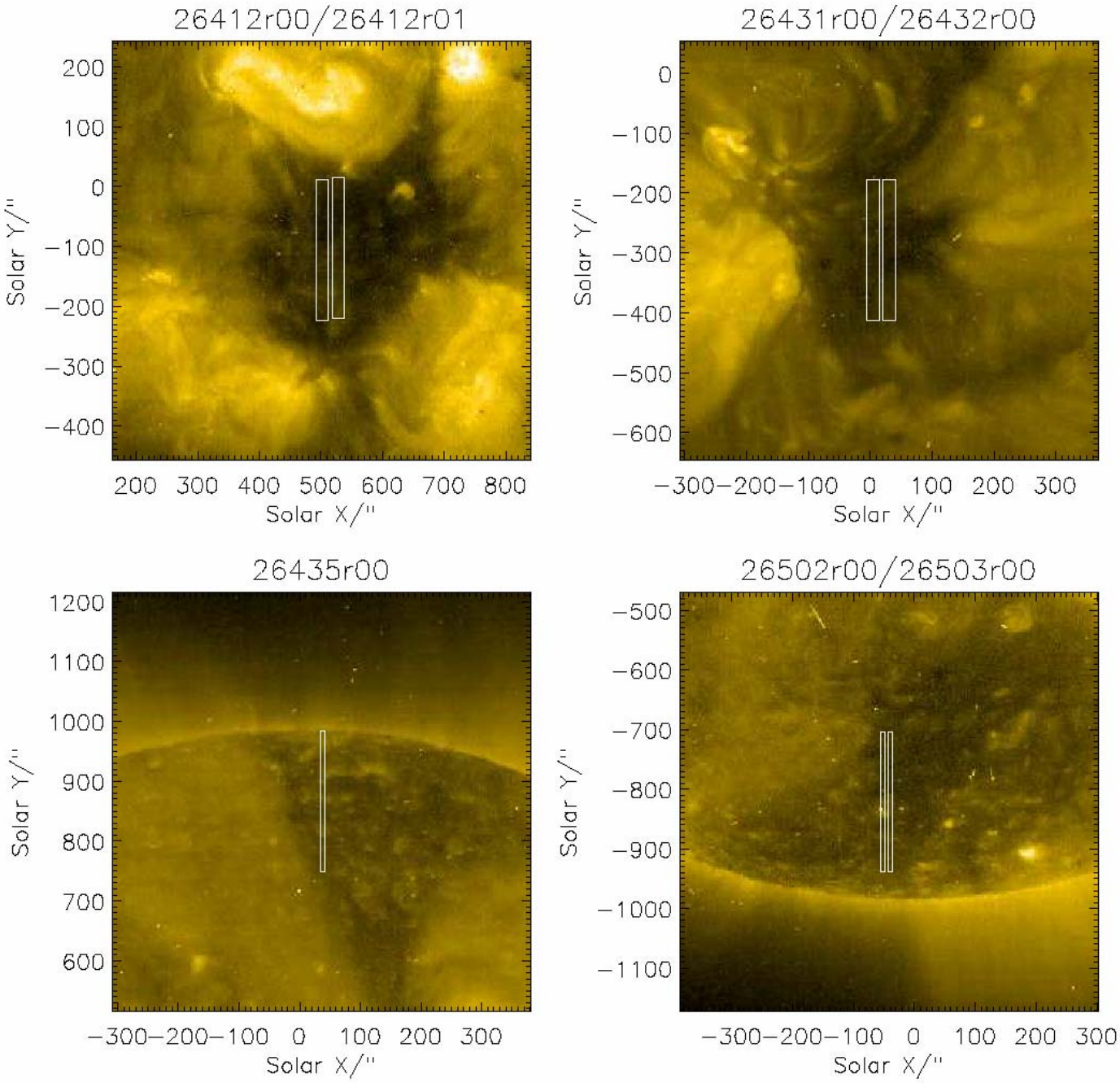
26412r00/26412r01
Solar Y/''
200
100
0
−100
−200
−300
−400
200 300 400 500 600 700 800
Solar X/''
26431r00/26432r00
Solar Y/''
0
−100
−200
−300
−400
−500
−600
−300−200−100 0 100 200 300
Solar X/''
26435r00
Solar Y/''
1200
1100
1000
900
800
700
600
−300−200−100 0 100 200 300
Solar X/''
26502r00/26503r00
Solar Y/''
−500
−600
−700
−800
−900
−1000
−1100
−300−200−100 0 100 200 300
Solar X/''

South Polar dataset

EIT 284 image Showing the Over-plotted slit position For the polar dataset

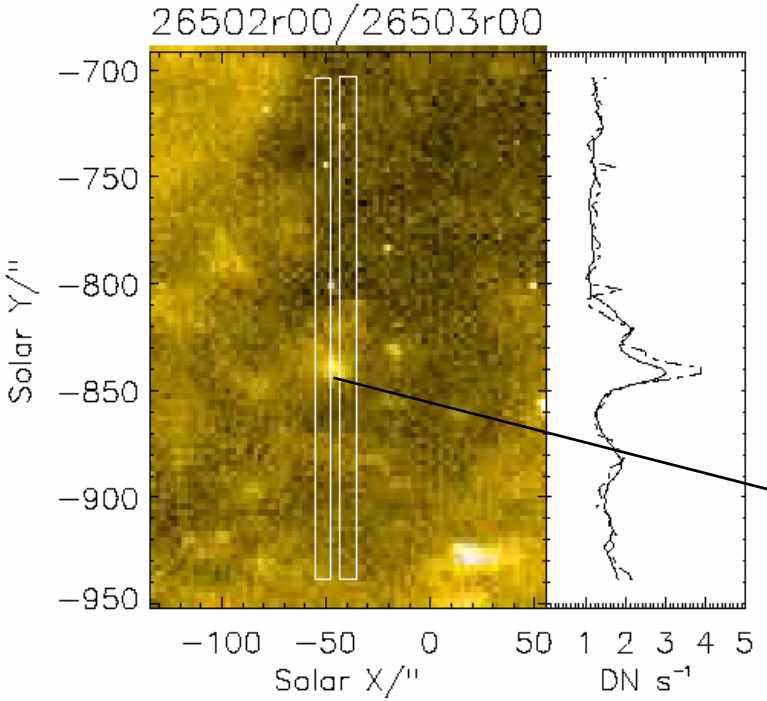

Bright point

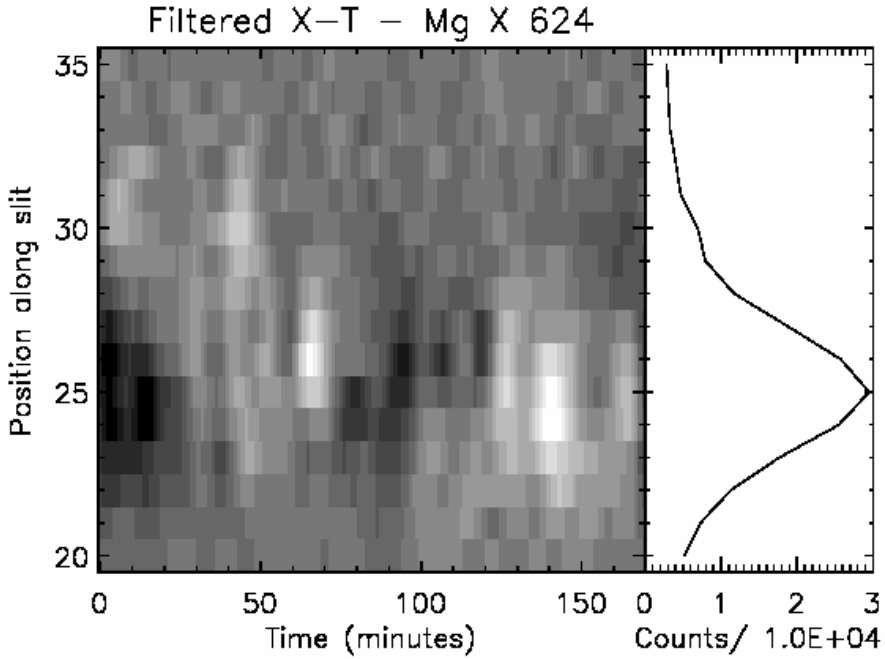

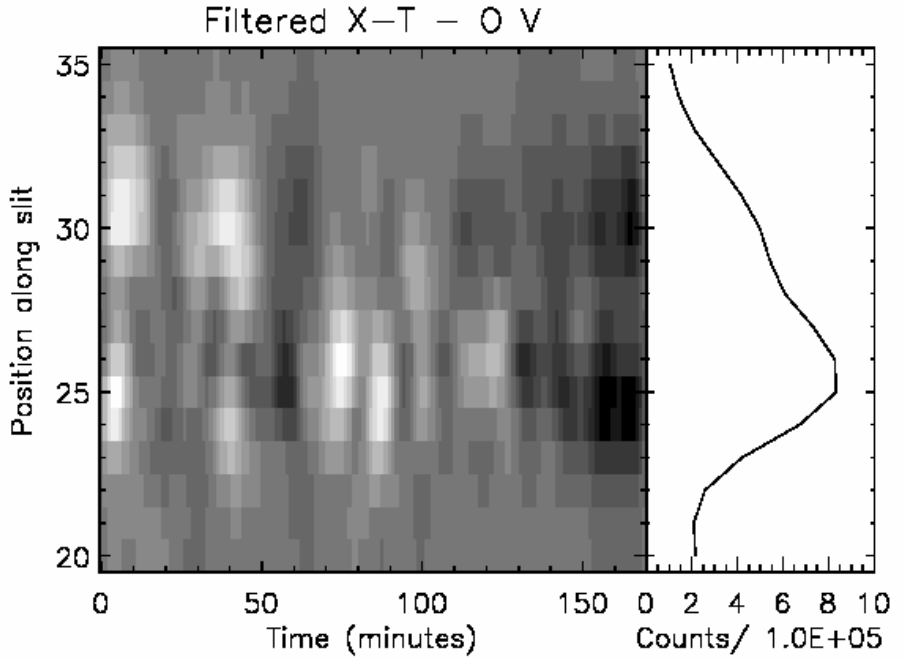

Wavelet results for px 26 (the bright one) in South polar CH

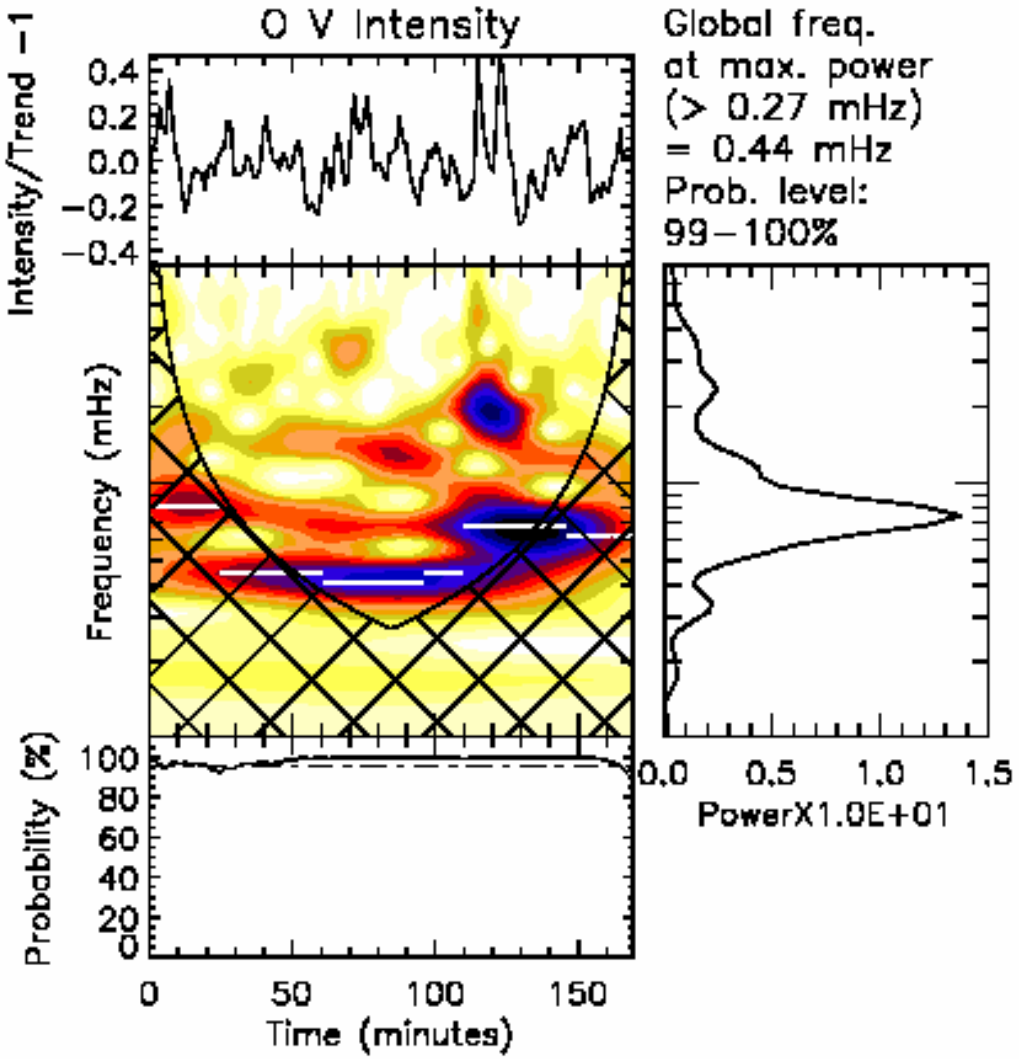

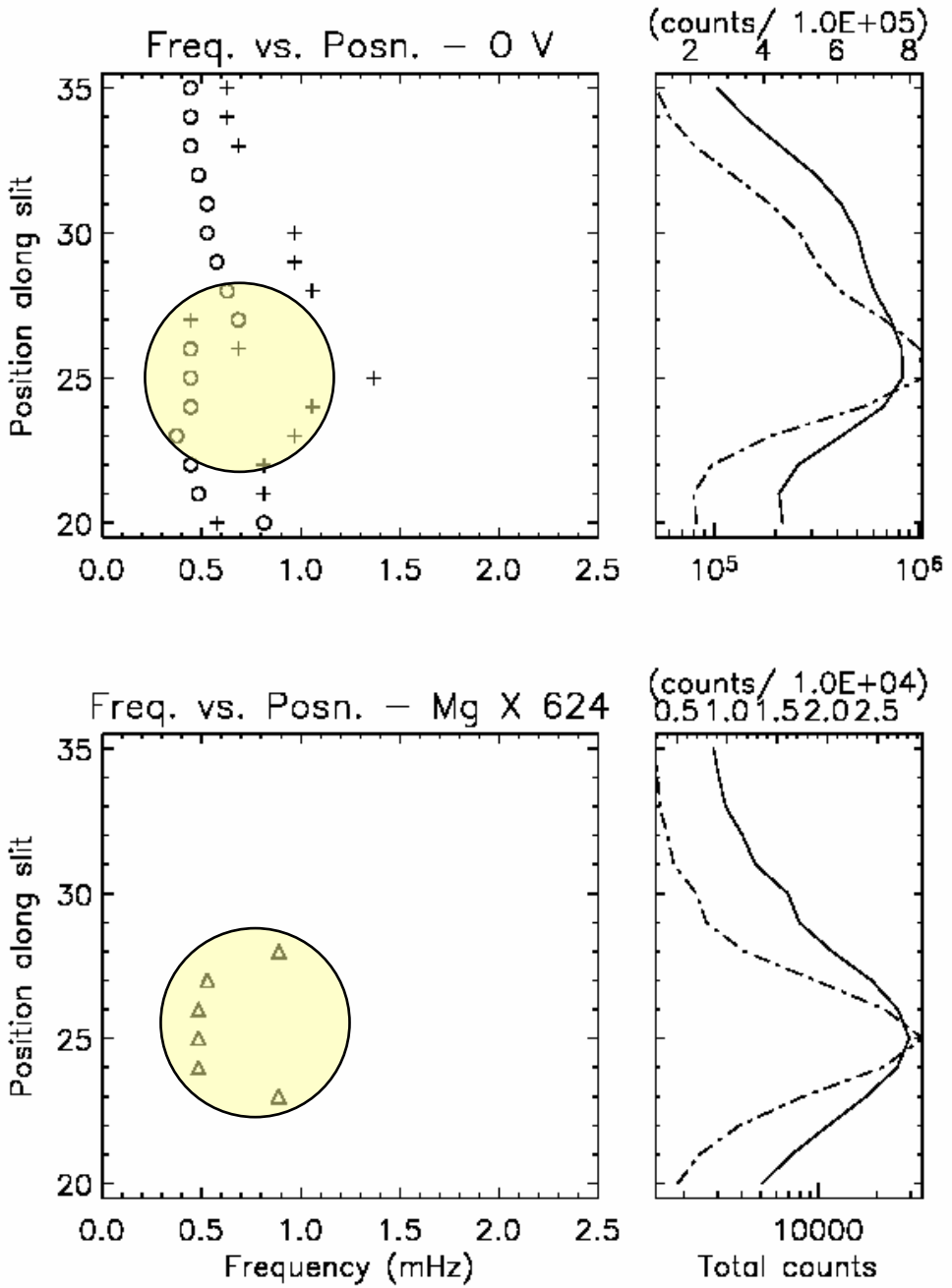

X-F slices
For a portion
of the
Slit in the
South polar
CH

Let us turn our attention to the Equatorial coronal hole Now....

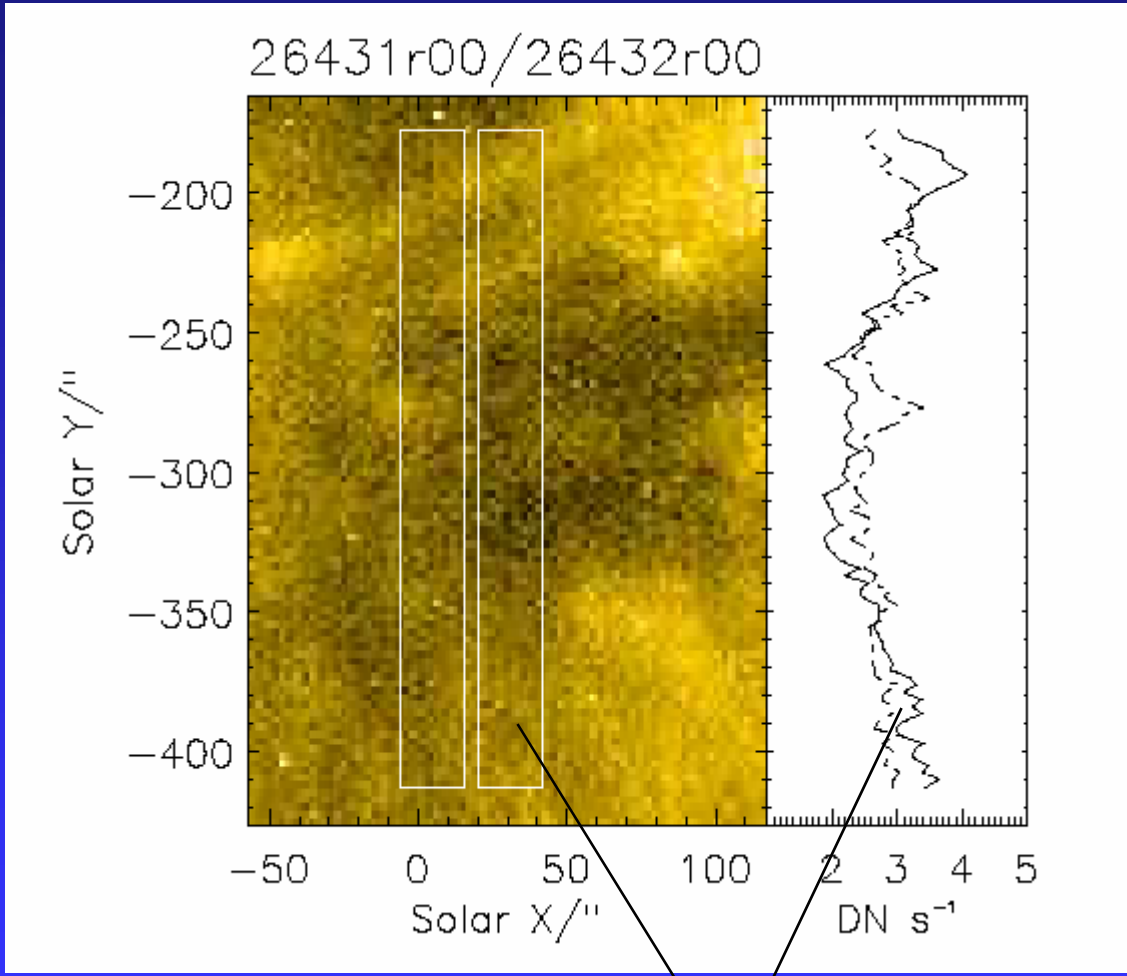

Px 8

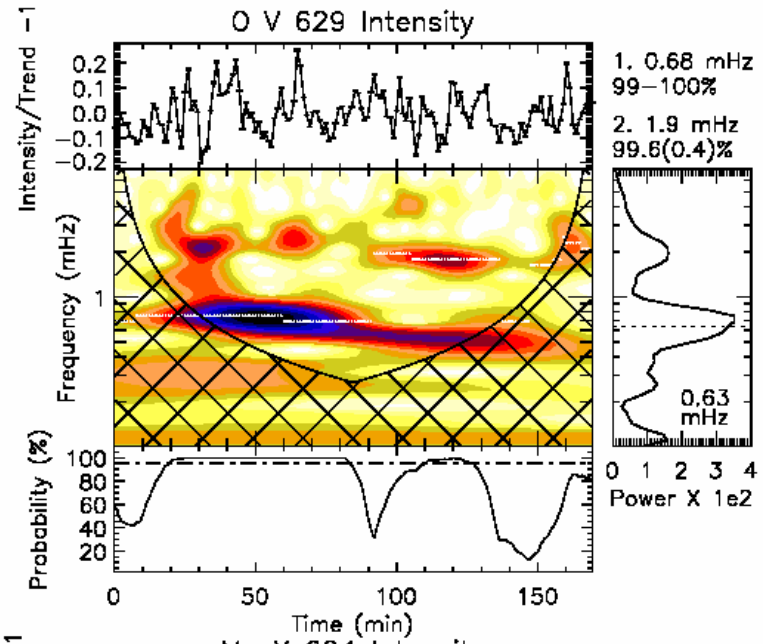
O V 629 Intensity
Intensity/Trend −1
Frequency (mHz)
Probability (%)
Time (min)
1. 0.68 mHz
99−100%
2. 1.9 mHz
99.6(0.4)%
0.63 mHz
Power X 1e2

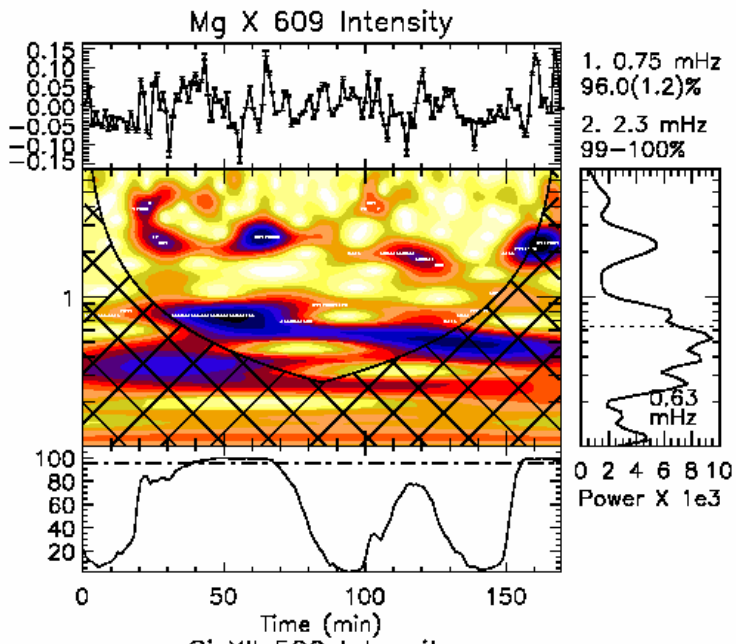
Mg X 609 Intensity
Frequency (mHz)
Probability (%)
Time (min)
1. 0.75 mHz
96.0(1.2)%
2. 2.3 mHz
99−100%
0.63 mHz
Power X 1e3

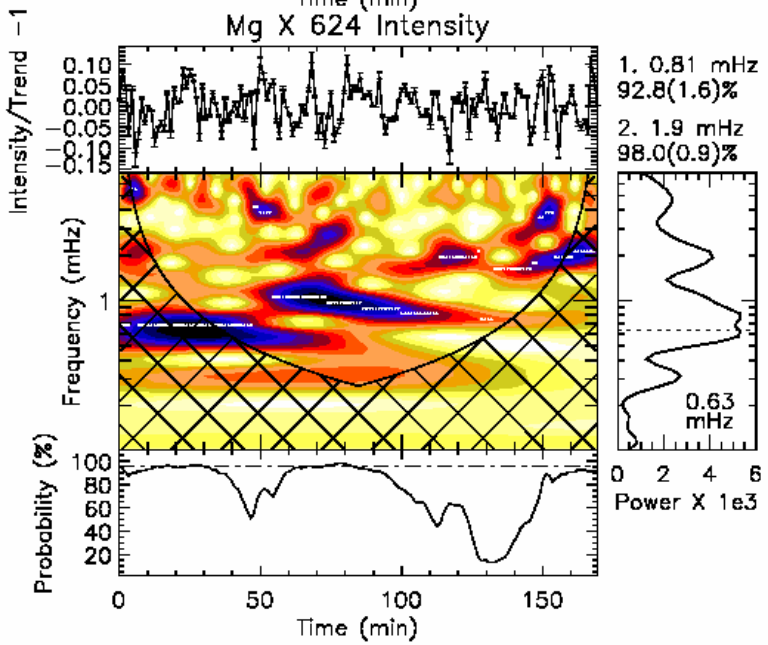
Mg X 624 Intensity
Intensity/Trend −1
Frequency (mHz)
Probability (%)
Time (min)
1. 0.81 mHz
92.8(1.6)%
2. 1.9 mHz
98.0(0.9)%
0.63 mHz
Power X 1e3

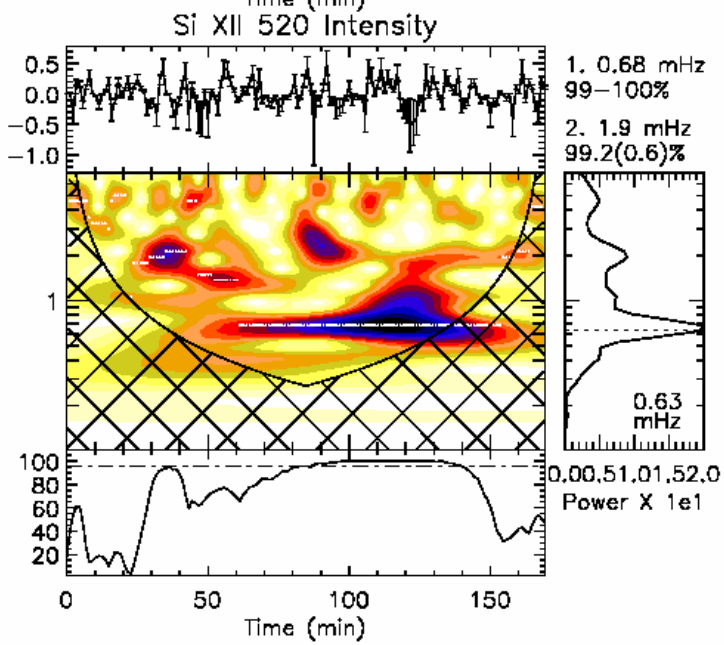
Si XII 520 Intensity
Frequency (mHz)
Probability (%)
Time (min)
1. 0.68 mHz
99−100%
2. 1.9 mHz
99.2(0.6)%
0.63 mHz
Power X 1e1

A statistical approach to measure time-delay

We follow the treatment of Athay & White (1979) Phase delay are plotted over the full -180^0 to $+180^0$ Range and as a function of frequency f. The Phase difference is given by,

$$\Delta\varphi = 2\,\Pi\,f\,T$$

Where T is the time-dealy, $\Delta\varphi$ will vary linearly with f and will change by 360^0 over freq interval

$\Delta f = 1/T$

Parrellel lines in $\Delta\varphi$ vs. F plots corresponding to fixed time-delay

Simulated data

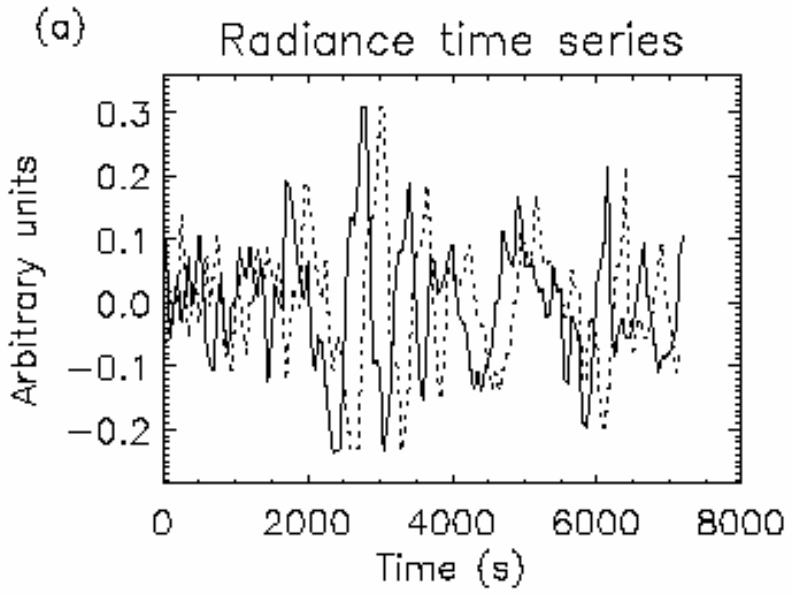

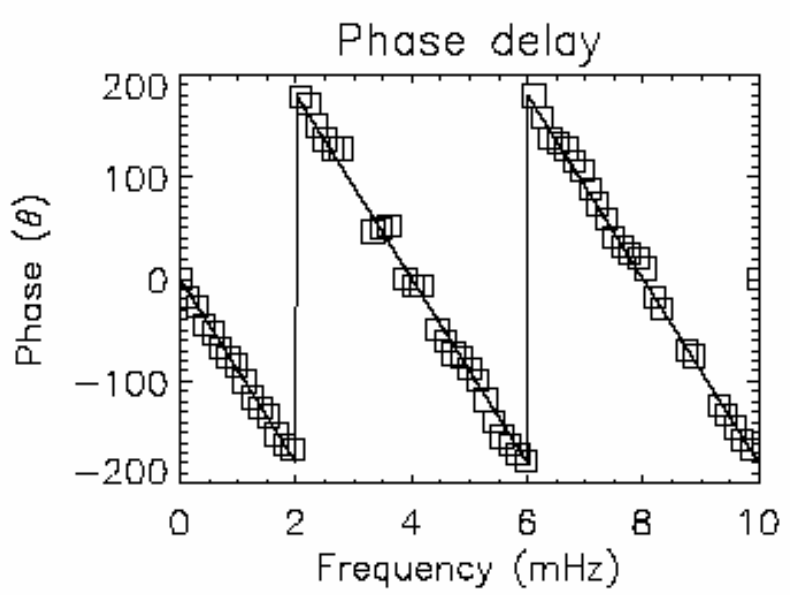

For a fixed time-delay of 250 s the calculated phase delays At frequencies squared symbols align themselves in Parrellel rows at 4 mHz intervals, as expected

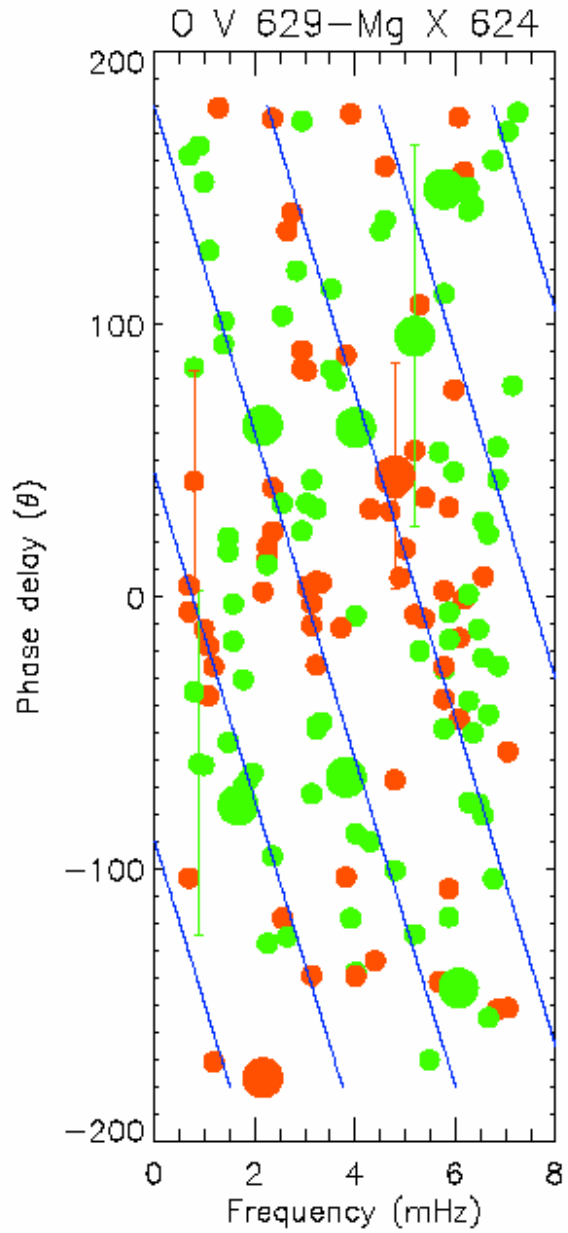

Dataset 26431-2
Equatorial CH

Time –delay 167 s

Height difference = 8937 Km

Phase speed = 54 km/s

Dataset 26502-3
Polar CH

Time –delay 100 s

Height difference = 8937 Km

Phase speed = 89 km/s

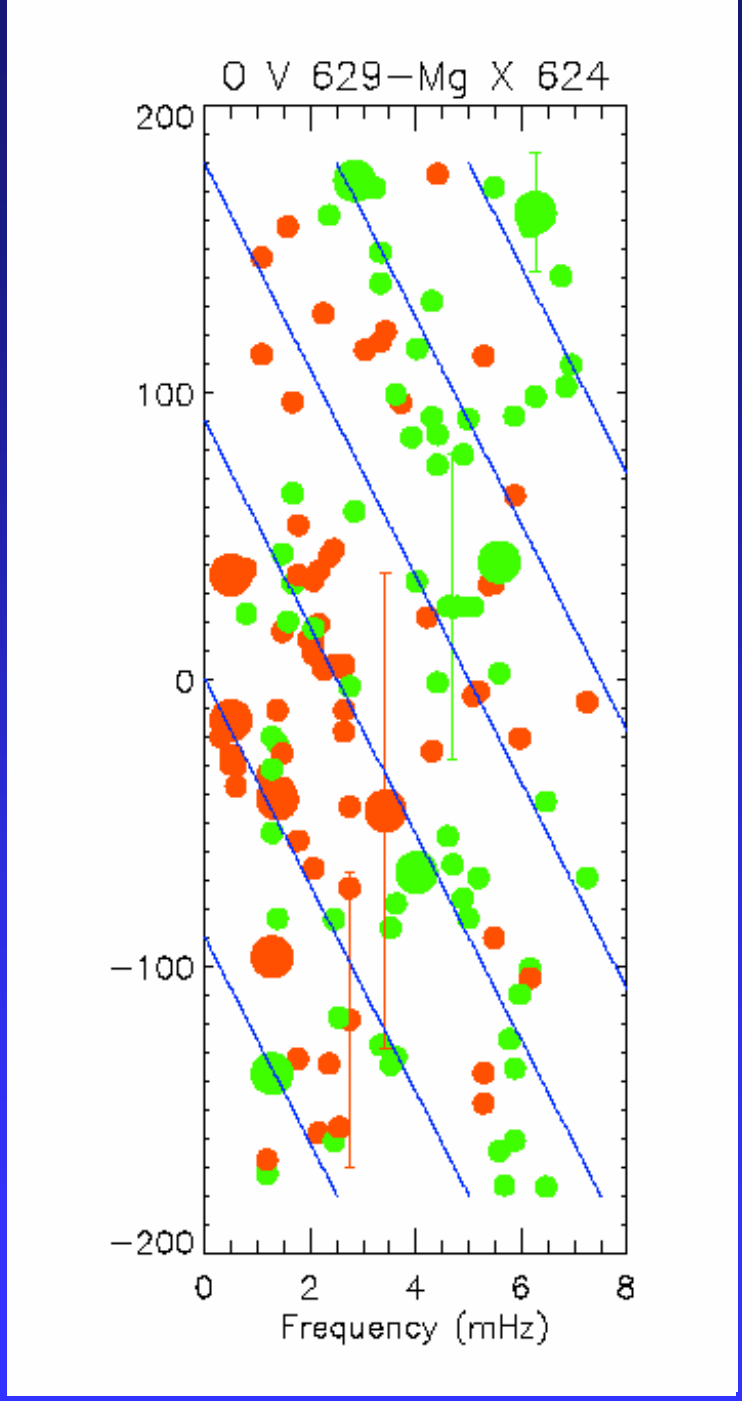

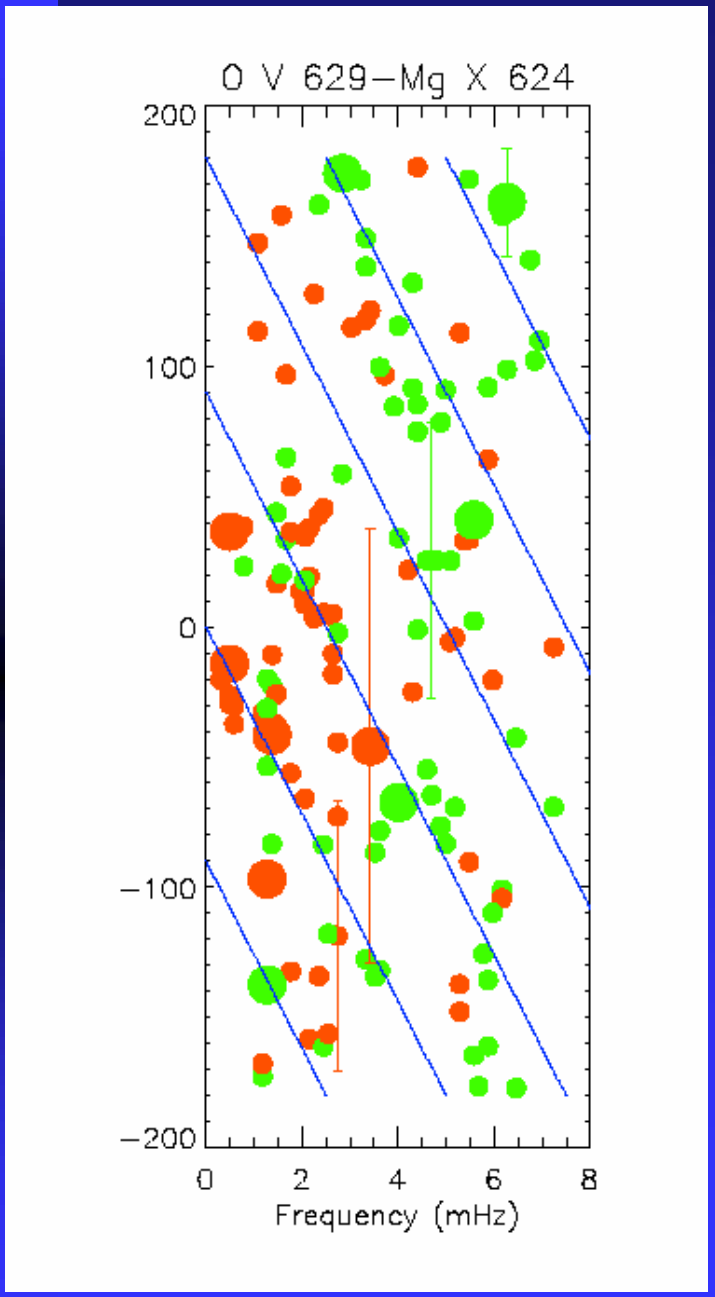

Polar CH with speeds 89 km/s

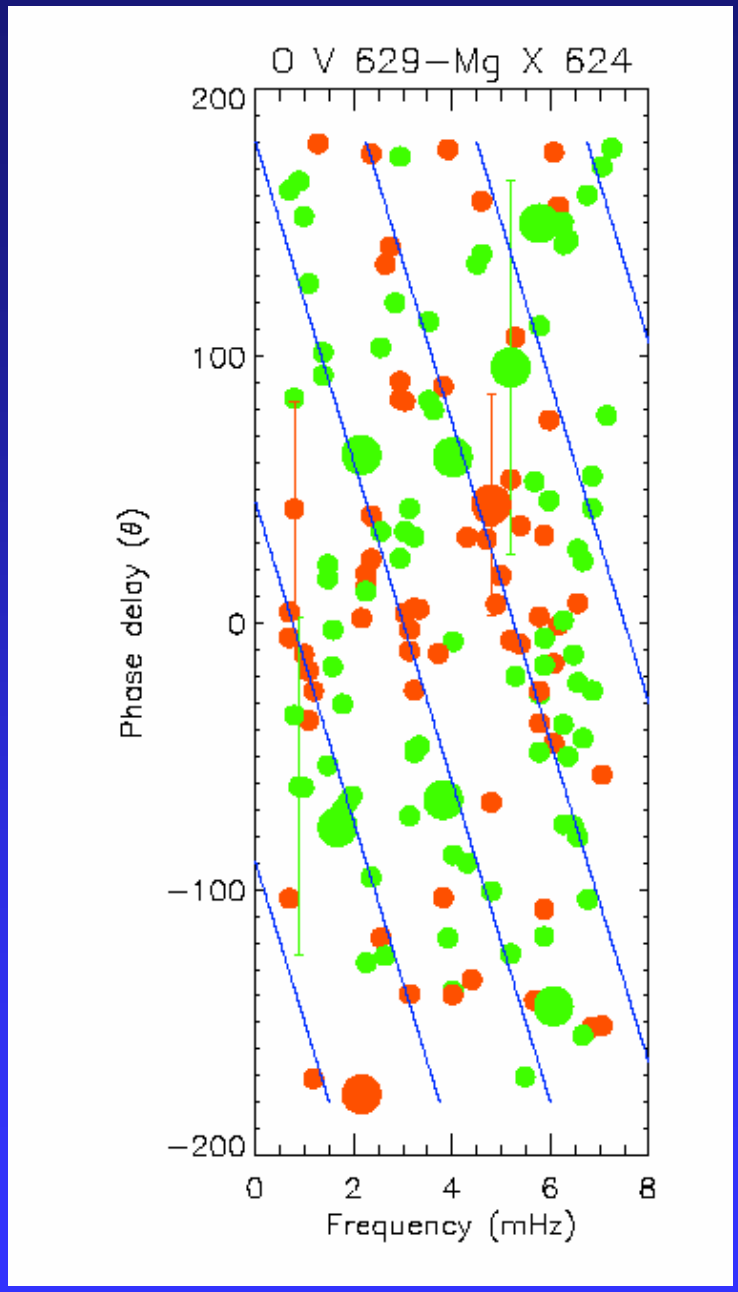

Equatorial CH 54 km/s

Conclusions:

- Detected presence of oscillations in CH with indications of prefered locations near bright points, presumably the base of the coronal funnels, network boundaries
- We find presence of upward propagating magnetoacoustic type waves, which has already been reported earlier
- Time-delay estimates gives phase speeds in the polar regions of the order of 90 km/s and in the equatorial regions abot 55 km/s (much slower!!)

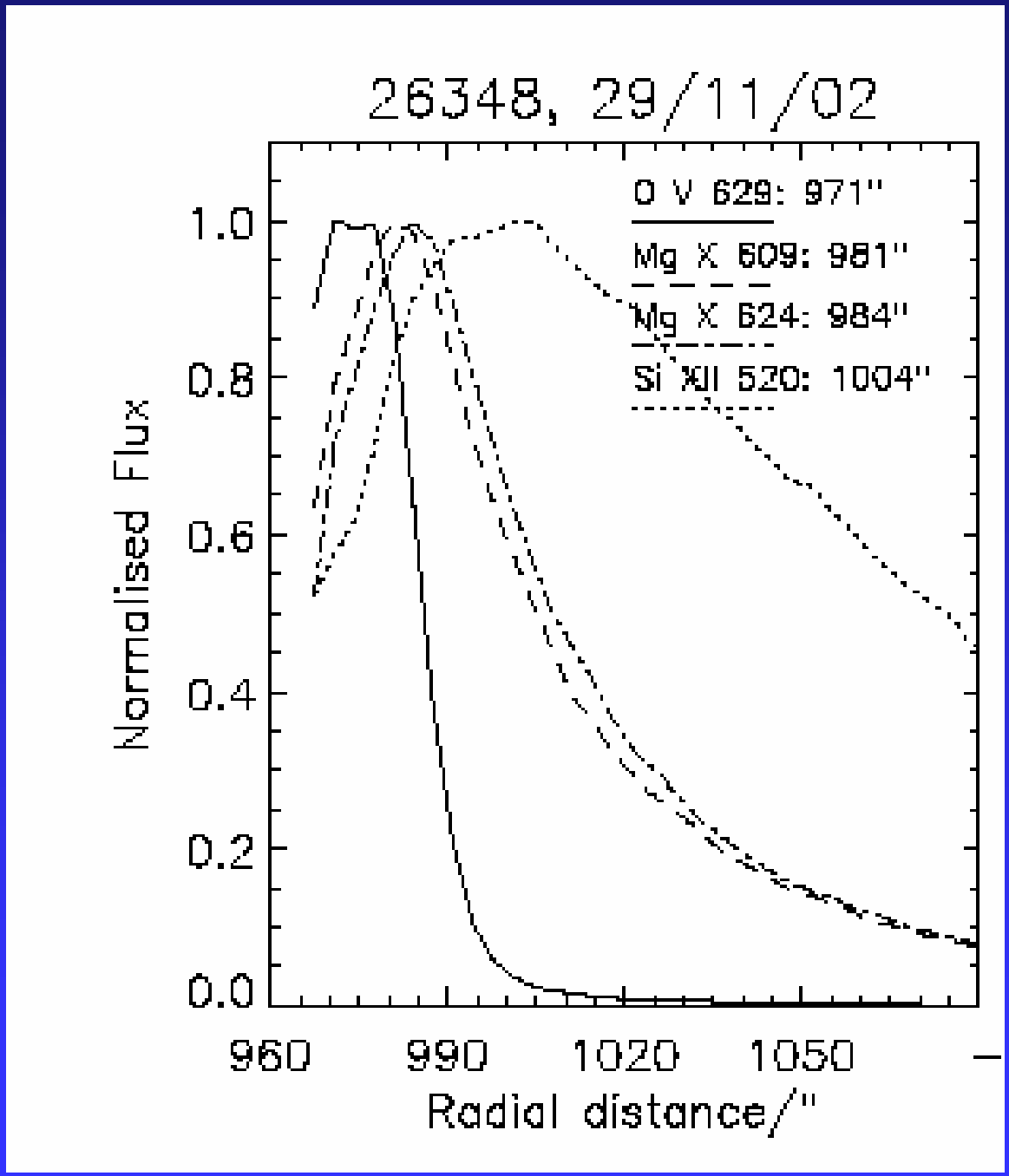
26348, 29/11/02
O V 629: 971"
Mg X 609: 981"
Mg X 624: 984"
Si XII 520: 1004"
Normalised Flux
1.0
0.8
0.6
0.4
0.2
0.0
960
990
1020
1050
Radial distance/"